

Evaluation of the effects of pulsed wave LLLT on tibial diaphysis in two rat models of experimental osteoporosis, as examined by stereological and real-time PCR gene expression analyses

Zhaleh Mohsenifar¹ · Mohammadjavad Fridoni² · Mahdi Ghatrehsamani³ ·
Mohammad-amin Abdollahifar⁴ · Hojjatallah Abbaszadeh⁴ ·
Atarodalsadat Mostafavinia⁴ · Somaye Fallahnezhad⁴ · Mohammadali Asghari⁵ ·
Saba Bayat⁶ · Mohammad Bayat⁴

Received: 14 December 2015 / Accepted: 19 February 2016 / Published online: 10 March 2016
© Springer-Verlag London 2016

Abstract Osteoporosis (OP) and osteoporotic fracture are major public health issues for society; the burden for the affected individual is also high. Previous studies have shown that pulsed wave low-level laser therapy (PW LLLT) has osteogenic effects. This study intended to evaluate the impacts of PW LLLT on the cortical bone of osteoporotic rats' tibias in two experimental models, ovariectomized and dexamethasone-treated. We divided the rats into four ovariectomized induced OP (OVX-d) and four dexamethasone-treated (glucocorticoid-induced OP, GIOP) groups. A healthy (H) group of rats was considered for baseline evaluations. At 14 weeks following ovariectomy, we subdivided the OVX-d rats into the following groups: (i) control which had OP, (ii) OVX-d rats treated with alendronate (1 mg/kg), (iii) OVX-d

rats treated with LLLT, and (iv) OVX-d rats treated with alendronate and PW LLLT. The remaining rats received dexamethasone over a 5-week period and were also subdivided into four groups: (i) control rats treated with intramuscular (i.m.) injections of distilled water (vehicle), (ii) rats treated with subcutaneous alendronate injections (1 mg/kg), (iii) laser-treated rats, and (iv) rats simultaneously treated with laser and alendronate. The rats received alendronate for 30 days and underwent PW LLLT (890 nm, 80 Hz, 0.972 J/cm²) three times per week during 8 weeks. Then, the right tibias were extracted and underwent a stereological analysis of histological parameters and real-time polymerase chain reaction (RT-PCR). A significant increase in cortical bone volume (mm³) existed in all study groups compared to the

✉ Mohammad Bayat
mohbayat@sbmu.ac.ir; bayat_m@yahoo.com

Zhaleh Mohsenifar
zmohsenifar@yahoo.com

Mohammadjavad Fridoni
fredoni_javad@yahoo.com

Mahdi Ghatrehsamani
mahdi.samani.2020@gmail.com

Mohammad-amin Abdollahifar
m_amin58@yahoo.com

Hojjatallah Abbaszadeh
hoomanabs@gmail.com

Atarodalsadat Mostafavinia
a.mostafavinia@gmail.com

Somaye Fallahnezhad
sfallahnejad@gmail.com

Mohammadali Asghari
mohammad.a.asghari@gmail.com

Saba Bayat
sababayat@gmail.com

- ¹ Pathology Department, Ayatollah Taleghani Hospital, Shahid Beheshti University of Medical Sciences, Tehran, Iran
- ² Department of Anatomy, School of Medicine, Zanjan University of Medical Sciences, Zanjan, Iran
- ³ Cellular and Molecular Biology Research Centre, Shahrekord University of Medical Sciences, Shahrekord, Iran
- ⁴ Department of Anatomical Sciences and Biology, School of Medicine, Shahid Beheshti University of Medical Sciences, PO Box: 19395/4719, Tehran 1985717443, Iran
- ⁵ School of Medicine, Shahid Beheshti University of Medical Sciences, Tehran, Iran
- ⁶ School of Medicine, Arak University of Medical Sciences, Arak, Iran

healthy rats. There were significant decreases in trabecular bone volume (mm^3) in all study groups compared to the group of healthy rats. The control rats with OP and rats from the vehicle group showed significantly increased osteoclast numbers compared to most other groups. Alendronate significantly decreased osteoclast numbers in osteoporotic rats. Concurrent treatments (compounded by PW LLLT and alendronate) produce the same effect on osteoporotic bone.

Keywords Osteoporosis · Glucocorticoid-induced osteoporosis · Low-level laser therapy · Ovariectomized induced osteoporosis · Biomechanical properties · Stereology · Real-time polymerase chain reaction

Abbreviations

OP	Osteoporosis
BMU	Basic multicellular unit
ECM	Extracellular matrix
TGF- β	Transforming growth factor beta
IGF-I	Insulin-like growth factor-I
BMPs	Bone morphogenetic proteins
GC	Glucocorticoid
GIOP	Glucocorticoid-induced osteoporosis
BMD	Bone mineral density
LLLT	Low-level laser therapy
LED	Light-emitting diode of Sohn et al. [15] study
CW	Continuous wave
PW	Pulsed wave
OVX-d	Ovariectomized induced OP
RT-PCR	Real-time polymerase chain reaction
cDNA	Complementary DNA
LSD	Least significant difference
GTP	Guanosine triphosphate
AlGaAs	Aluminum gallium arsenide

Introduction

Osteoporosis (OP), a common bone disease is characterized by reductions in bone density and deterioration of bone structure [1]. Osteoporosis and osteoporotic fracture are major public health issues for society; the burden for the affected individual is also high [2], potentially leading to bone fractures and their resultant complications. The most common fractures are those of the vertebrae, proximal femur (femoral neck), and distal forearm (wrist) [3]. Hip fractures impose an excess annual mortality rate of 8 to 36 % [4]. Postmenopausal estrogen deficiency is the cause of OP type I, which is the most prevalent form of the disease [5]. The reduction in bone mass that occurs during estrogen deficiency has long been regarded as the critical event leading to bone fracture.

Microarchitecture describes the microscopic structure and morphology of trabecular and cortical bones. It is characterized using bone histomorphometry and micro-CT scanning (μCT). Osteoporotic fractures are believed to occur when both the bone mass and the microarchitecture of the bone degrade to such an extent that bone strength is reduced. These fractures occur under normal physiological loads [6]. Evidence suggests that estrogen-deficient states lead to increased microdamage [7]. Osteoblasts and osteoclasts, together referred to as the basic multicellular unit (BMU), regulate bone remodeling. Having estrogen receptors, osteoclasts trigger protein synthesis when activated by estrogen [8]. Estrogen has an inhibitory effect on osteoclasts as the proteins produced following estrogen binding inhibit bone resorption by decreasing the formation of mature osteoclasts [8] and increasing osteoclast apoptosis [9]. When estrogen levels are deficient, the number of hematopoietic progenitors increases. Because they possess estrogen receptors [8], the normal function of osteoblasts and osteocytes is affected during estrogen-deficient states such as during the post-menopausal period.

A number of cytokines and growth factors govern the activity of bone cells during normal bone remodeling. The extracellular matrix (ECM) releases factors such as transforming growth factor beta (TGF- β) and insulin-like growth factor-I (IGF-I) during bone resorption. These factors recruit and activate osteoblasts to begin collagen synthesis. Collagen type 1 is involved in skeletal development and has regulatory effects on bone cells [10]. The process of osteoblast maturation is affected by the action of various endocrine, paracrine, and autocrine factors. These factors include a number of bone morphogenetic proteins (BMPs) and IGF-I. Medically administered to facilitate spinal fusion, the recombinant human BMP-2 is approved for OP therapy [11].

Glucocorticoid (GC)-induced osteoporosis (GIOP) is the most common cause of secondary OP [12]. Bisphosphonates are first-line prophylactic agents for GIOP. The bisphosphonates, alendronate and risedronate, both increase the bone mineral density (BMD) of the spine and hips and reduce the vertebral fracture rate [13]. Treatment with anabolic agents such as low-level lasers strongly stimulates bone turnover and seems to be superior to treatment with alendronate [12, 13].

Prevention of OP and its complications is an essential socioeconomic priority [14]. Numerous treatments exist and include estrogen therapy, bisphosphonate compounds, physical activity programs, and low-level laser therapy (LLLT).

One study showed that light-emitting diode (LED) irradiation downregulated osteoclastogenesis by reducing ROS production. The authors concluded that LED irradiation or LLLT might be useful as an alternative, conservative approach to OP management [15]. Kiyosaki et al. reported that continuous wave (CW) LLLT increased the production of IGF-I and BMP, which stimulated bone

mineralization [16] and significantly stimulated the number and area of bone nodules [17].

The benefits of LLLT for treatment of OP are controversial. Several studies have reported positive effects of LLLT on ovariectomized induced OP (OVX-d) rats [18–20], whereas others found no improvement in OVX-d and GIOP OP models that underwent LLLT [21–23].

To the best of our knowledge, no study has been performed that investigates the effects of pulsed wave (PW) LLLT on stereological analysis of histological parameters and gene expression methods in the tibias of OVX-d and GIOP rats. Paraclinical information such as BMD, biochemical markers, histological parameters, and gene expression findings can assist clinicians in determining the treatment of choice in patients with OP [24]. This study intends to evaluate the impacts of PW LLLT on cortical bone in two experimental rat models of OP.

We conducted a stereological analysis of histological parameters by measuring total bone volume, cortical bone volume, trabecular bone volume, and total bone marrow volume. The numbers of osteocytes, osteoblasts, and osteoclasts were counted by stereological techniques. TGF- β , IGF-I, BMP-2, and type 1 collagen gene expressions were measured using the real-time polymerase chain reaction (RT-PCR) method.

Materials and methods

Animals and study design

Both male and female Wistar rats were housed in standard rat cages. Rats were maintained on a 12-h light/dark schedule and provided water ad libitum. All procedures were approved by the Medical Ethics Committee at Shahid Beheshti University of Medical Sciences, Tehran, Iran (protocols no.: 1393-1-91-1350 and 1392-1-115-1160). The rats' body weights were monitored weekly, and the volume of drugs administered was calculated according to the most recent body weight. In this study, OVX-d and GIOP rats tibias received PW LLLT and alendronate. These rats subsequently underwent a stereological analysis of histological parameters and RT-PCR gene expression evaluation methods. The healthy (H) group (group 5) comprised six normal rats which were used for the baseline studies.

Sampling of the OVX-d and GIOP groups

We randomly divided 48 rats into eight groups of 6 rats per group as follows: four groups of OVX-d rats and four groups that received dexamethasone (GIOP). Ovariectomies were performed while rats were under general anesthesia, via two paravertebral skin incisions. The uterine tubes were ligated, and after removal of the ovaries, we closed the incisions. Rats

received antibiotic therapy with ceftriaxone (50 mg/kg) immediately before and 24 and 48 h after surgery [23]. All animals were kept for 98 days after surgery in cages to allow for the development of OP [25]. At the end of this period, the rats were submitted to the following treatments: group 1 (OC) comprised control rats with OP, group 2 (OA) were OVX-d rats treated subcutaneously with 1 mg/kg alendronate (Alborz Darou Co., Tehran, Iran), group 3 (OL) consisted of OVX-d rats that received PW LLLT three times weekly (Table 1), and group 4 (OAL) were OVX-d rats treated with PW LLLT and concomitant administration of alendronate (1 mg/kg).

The remaining rats received a daily intramuscular (i.m.) dose of dexamethasone (1 mg/kg; Alborz Darou Co., Tehran, Iran), administered 6 days per week for 5 weeks [26]. After 5 weeks, dexamethasone-treated rats were subdivided into four groups: group 6 (control) consisted of OP rats treated with i.m. injections of vehicle (distilled water, DC), group 7 (DA) or GIOP rats received subcutaneous alendronate injections at a dose of 1 mg/kg (Alborz Darou Co., Tehran, Iran) [27], group 8 (DL) consisted of GIOP rats treated with PW LLLT (Table 1) three times per week, and group 9 (DAL) consisted of GIOP rats treated with PW LLLT and concomitant administration of 1 mg/kg/day alendronate. In the laser groups, both tibias (four points each) were completely radiated with the laser probe held vertically to the bone from a distance of less than 10 mm. For 2 months, the rats received PW LLLT. Rats received alendronate injections for 30 days. At 2 months after the beginning of the treatments, all rats were sacrificed with an overdose of anesthesia. The right tibias were extracted for histological examination, and the left tibias were frozen at -80°C for further RT-PCR gene expression analyses.

Histological and stereological examinations

The bones were fixed in formalin saline and decalcified in EDTA for a duration of 56 days, right after biomechanical examination [23]. The primary volume V (primary) of the

Table 1 Specifications of the laser used

Parameters	Dose and unit
Peak power output	75 W
Average power	1.08 mW
Power density	1.08 mW/cm ²
Wave length	890 nm
Pulse frequency	80 Hz
Spot size	1 cm ²
Pulsed duration	180 ns
Duration of exposure for each point	900 s
Energy density	0.972 J/cm ²

tibias was measured using the immersion method [28]. Then, the tibia was embedded in paraffin blocks and cut longitudinally into 5 and 25- μm -thick sections with a microtome. For a microscopic descriptive analysis of each group, slides were prepared by using hematoxylin and eosin (H&E) dyes. All measurements were performed using a magnifying objective ($\times 4$, $\times 40$) (Fig. 1).

Stereological study

Measurement of bone volume

Using a projecting microscope, the live image of each tibial bone section was evaluated. Following this procedure, eight to ten sections were obtained and analyzed for each tibial bone. The volumes (V) were calculated using the Cavalieri method. Using the stereological software, a grid of points was superimposed on the images. The volume of the tibial bone was estimated by the following formula:

$$V(\text{bone}) = \Sigma p \times a/p \times t$$

where Σp is the total points hitting the tibial bone sections, a/p is the area associated with each point, and t is the distance between the sampled sections [29, 31].

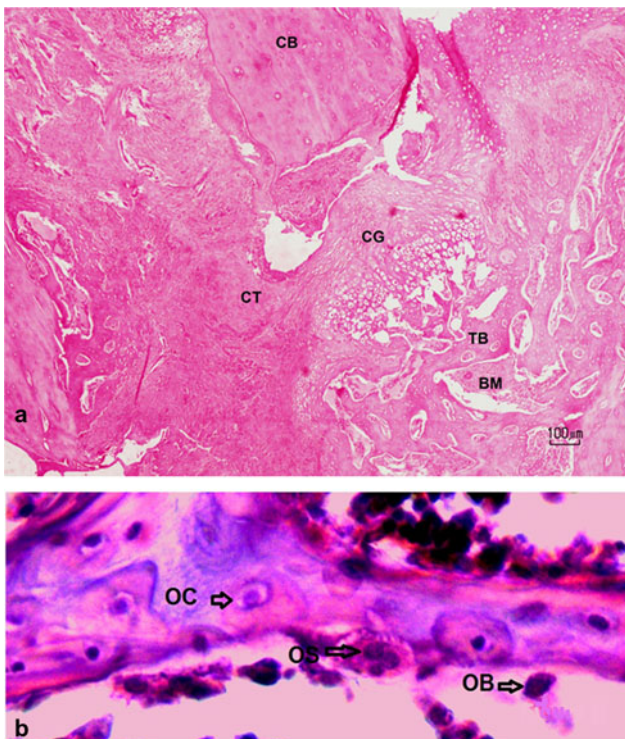


Fig. 1 Light micrograph of stereological examination of bony tissues (a) and cells (b) (H&E)

Estimation of the number of the bone cells

For estimation of numerical density and total number of the bone cells, a dissector method was used. The specimens were evaluated at $\times 40$ magnification with high numerical aperture. An image was captured and sent to the image analysis computer. The focus plane was set at the surface of the specimen. Then, a set of three unbiased measurement frames was superimposed on the live image. At the same time, the microcator measuring the optical distance through the specimen in the z -axis was zeroed. By gently moving the focus down through the specimen, an approximately 0.5-mm-thin focal plane made objects come into focus and disappear. Bone cells falling in the measurement frames' permitted areas were counted as they came into focus until the microcator indicated that the focal plane had traveled 10 μm through the specimen. The numerical density of cells is obtained by

$$Nv = (\Sigma Q- / (h \times a/f \times \Sigma p)) \times (t/BA)$$

where $\Sigma Q-$ is the number of the whole cells counted in all the dissectors, h is the height of the optical dissector, a/f is the area of the counting frame, Σp is the total number of the counted frames, BA is the microtome block advance to cut the block (25 μm), and t is the mean of the final section thickness (20 μm). To estimate the total number of the bone cells, the following formula was used: $N(\text{bone cell}) = Nv \times V(\text{final})$ [30, 31].

RNA extraction

Frozen bones crushed by Chinese Haven were homogenized in TRIzol (Invitrogen, USA) using a tissue laser instrument (Qiagen, GmbH). The total RNA was purified.

We added 200 μL of chloroform (Merck, Germany) to the resultant TRIzol mixture; the samples were shaken vigorously and incubated at room temperature for 5 min. Samples were centrifuged at 10,000 RPM for 20 min at 4 $^{\circ}\text{C}$. The separated, colorless aqueous layer was mixed with 0.5 mL of isopropanol. The samples were centrifuged again at 10,000 $\times g$ or 10,000 RPM for 20 min at 4 $^{\circ}\text{C}$. The pellet was resuspended in 1 mL ethanol and centrifuged at 12,000 RPM for 20 min at 4 $^{\circ}\text{C}$. The resultant pellet was dried for 10 min at room temperature. Nuclease-free deionized water (50 μL) was added, and the RNA concentration was estimated by UV spectrophotometry at a 260 nm wavelength. Purity was assessed by the A260/A280 ratio and A260/A230 ratio.

Prior to reverse transcription, the sample was treated with RNase-free DNase I (Takara Bio Inc., Japan) to remove any contaminating DNA. For RT-PCR, 1 μg total RNA was reversely transcribed to complementary DNA (cDNA) with oligo(dT) and random hexamer primers using 1 unit/mL M-

MLV reverse transcriptase (Invitrogen, CA, USA) at 95 °C for 15 min and 42 °C for 45 min.

RT-PCR

The expression of the candidate gene development was analyzed using quantitative RT-PCR with the SYBR® Green Real-time PCR Master Mix (Takara Bio, Inc.). Table 2 shows the oligonucleotide primers.

For each sample, three replicates for each target gene were performed in a final volume of 20 µL that contained 10 µL of 2× SYBR® Green PCR Master Mix, 1 µL cDNA, 2 µL of the forward and reverse primers, and 7 µL of water. Thermo cycling conditions were as follows: an initial denaturation at 95 °C for 2 min, followed by 35–40 cycles of 92 °C for 15 s, 60 °C annealing for 30 s, and a 72 °C extension for 45 s.

The specificity of the PCR amplification procedures was checked with melting curves. Quantification of the relative changes in gene expression was performed using the 2^{-ΔΔCt} method [32]. The mRNA levels of candidate genes were normalized to the signal for 18s rRNA.

Statistical analysis

All data were expressed as mean ± standard errors of mean (SEMs). Normal distribution of data was analyzed using the Shapiro test. Parametric and nonparametric statistical methods were used. The one-way analysis of variance (ANOVA) test was used to compare changes among groups with normal distribution of data, and the least significant difference (LSD) test was used to identify differences. A *p* value of ≤0.05 was considered statistically significant. Nonparametric methods were used for statistical analysis of the other groups. These data were analyzed using the Kruskal-Wallis and Mann-Whitney *U* tests. Differences were regarded as significant if *p* < 0.005 for analyses between groups 1 and 9. The differences were also regarded as significant if *p* ≤ 0.01 for analyses between groups 1 and 5 and analyses between groups 5 and 9, respectively.

Table 2 Primers of the selected genes for quantitative real-time PCR

Gene	Gene ID	Primer sequences
TGF-beta1	NM_021578.2	Forward: 5' TAGCAACAATTCCTGGCGTTAC Reverse: 5' CCTGTATTCCGTCTCCTTGGTTC
IGF-1	NM_001082478.1	Forward: 5' GGAACATAAGGCACGCTGAAC Reverse: 5'TGAGGAAGCAGGTAGATGGTGA
BMP-2	NM_017178.1	Forward: 5' AGAAGCCAGGTGTCTCCAAGA Reverse: 5' CCACATCACTGAAGTCCACATACA
Type 1 collagen	NM_053304.1	Forward: 5' GGAGCAGCAAGAGCAAGGAG Reverse: 5' ACAGCAGGCGTAGGAAGGTC

Results

We reported tibial weight changes in our previous paper [24].

Stereological analyses

The results of stereological analyses are shown in Figs. 2, 3, 4, 5, 6, 7, and 8.

In terms of total bone volume, the LSD test showed a significant decrease in total bone volume in the OC group compared to all groups with the exception of groups DC and H (Fig. 2).

Significant increases existed in cortical bone volume (mm³) in all study groups compared to the H group (Mann-Whitney test), with *p* = 0.004 for the OC, OA, OL, DC, DA, and DAL groups and *p* = 0.008 for the OAL and DL groups. We observed a significant increase in osteoblasts in the DL group compared to the OC group (*p* = 0.004; Fig. 3).

A significant decrease existed in trabecular bone volume (mm³) in all study groups compared to the H group (Mann-Whitney test), with *p* = 0.004 for the OC, OA, OL, DC, DA, and DAL groups and *p* = 0.008 for the OAL and DL groups (Fig. 4).

In terms of total bone marrow, the OC group showed the lowest bone marrow volume among the studied groups. Significant differences existed between the OC group and the DC (Mann-Whitney test, *p* = 0.004), OA (LSD test, *p* = 0.037), and OL (LSD test, *p* = 0.015) groups (Fig. 5).

According to the LSD test, we observed significant decreases in osteocyte numbers in the OA (*p* = 0.05), OC (*p* = 0.008), OL (*p* = 0.000), and OAL (*p* = 0.019) groups compared to the H group. The dexamethasone-treated rats showed a significant increase in osteocyte numbers compared to the OVX-d rats, as seen in Fig. 6.

According to the Mann-Whitney test, there were significant decreases in osteoblast numbers in the OA (*p* = 0.008), OC (*p* = 0.004), and OL (*p* = 0.004) groups compared to the H group. The DA, DL, and DAL groups showed significant

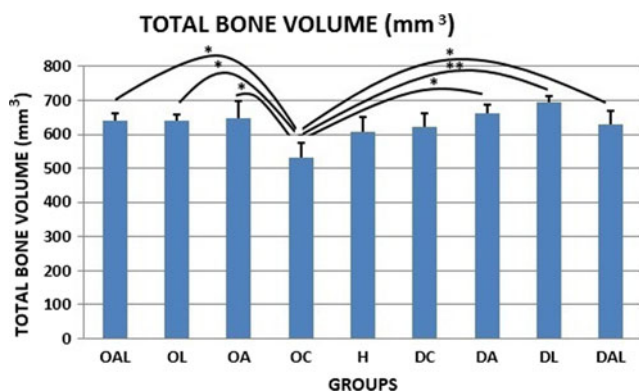


Fig. 2 Mean \pm SEM of the total bone volume (mm^3) of the studied groups compared by LSD test ($*p < 0.05$; $**p < 0.01$): ovariectomized (OVX-d) control rats (OC), OVX-d rats treated with alendronate (OA), OVX-d rats treated with LLLT (OL), OVX-d rats treated with LLLT and alendronate (OAL), healthy rats (H), dexamethasone-treated control rats (DC), dexamethasone-treated rats that received alendronate (DA), dexamethasone-treated rats that received LLLT (DL), and dexamethasone-treated rats that received alendronate and LLLT (DAL). LSD test showed that there was a significant decrease in the total bone volume of the OC group compared to all other groups except groups DC and H

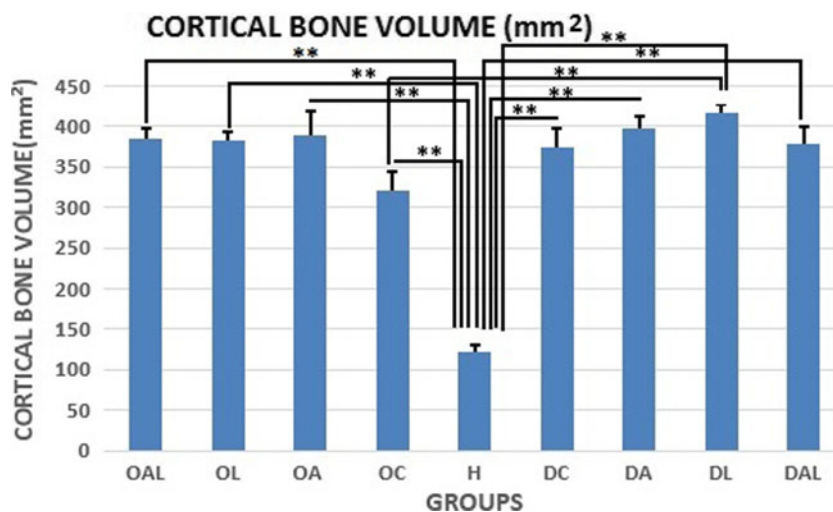
increases in osteoblasts compared to the OC, OA, and OL groups. Figure 7 shows the significant differences.

The H group had the lowest number of osteoclasts among the studied groups. The OC and DC groups showed significant increases in osteoclast numbers compared to most other groups (Fig. 8).

RT-PCR analysis

RT-PCR analysis results showed no significant differences in mRNA gene expressions of TGF- β , IGF-I, BMP-2, and type 1 collagen among the studied groups (Fig. 9).

Fig. 3 Mean \pm SEM of the cortical bone volume (mm^2) of the studied groups compared by Mann-Whitney test; $**p < 0.01$. There was a significant increase in the cortical bone volume in all study groups compared to the healthy group



Discussion

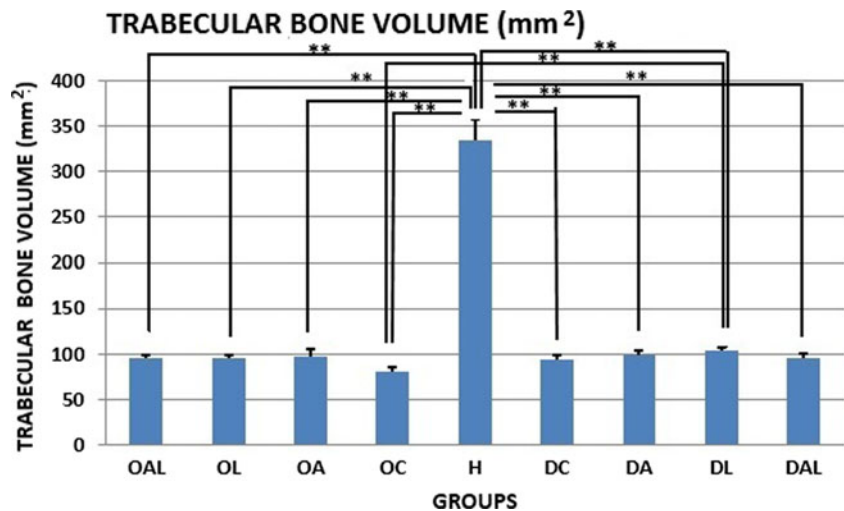
In the current study, ten sections were sampled starting with a random number between 1 and 10 and about eight to ten sections in each animal were selected in a systematic random manner.

After that, the microcator was attached to the stage of the microscope to measure the z-axis traveling. At the same time, the microcator measuring the optical distance through the specimen in the z-axis was zeroed. The upper and lower guard zones were used to avoid cutting artifacts that occurred at the upper and lower surfaces of the tissue sections. The height of the dissector was defined as the section thickness excluding the 5- μm -thick guard zone at the upper and lower of each section. Our study has shown the changes in the total volume and total number of the bone cells in tibial diaphysis in two rat models of experimental osteoporosis by using stereological methods. The advantage of using stereological methods is obtaining unbiased and precise estimations. The volume of the trabecular bone and bone cells in the different structures of the tibial diaphysis was estimated in advance.

The current study showed that both models of OVX-d and GIOP experimental OP significantly decreased trabecular bone volume, total bone marrow volume, and osteocyte and osteoblast numbers compared to healthy rats. There were also significant increases in cortical bone volume and osteoclast numbers compared to the group of healthy rats. However, the detrimental effects of an ovariectomy procedure on bone were more serious than dexamethasone administration.

Our results have shown an increase in cortical bone production. In post-menopausal osteoporotic women, an upregulation of both bone formation and resorption occurs [13]. Likewise, OP in OVX-d rats is associated with increased turnover due to increased resorption that exceeds bone formation [33]. This is attributed to the direct effect of estrogen on

Fig. 4 Mean \pm SEM of the trabecular bone volume (mm^3) of the studied groups compared by Mann-Whitney test; $**p < 0.01$. There was a significant decrease in the trabecular bone volume in all study groups compared to the healthy group



calcium absorption resulting in a direct influence on bone turnover [34].

We have found a significant decrease in trabecular bone volume in both the OVX-d and GIOP groups compared to the healthy rats. Approximately 80 % of the total skeleton is composed of cortical bone and the rest is comprised of trabecular bone. Certain regions of the skeleton are rich in trabecular bone. These areas include the vertebrae, femoral neck, and distal radius [35]. After menopause, there is a rapid loss of trabecular bone [36]. We have observed that GC changed the trabecular bone's properties and matrix composition. There were also increased trabecular surface remodeling and trabecular bone structure deterioration [36, 37].

In this study, cortical bone volume significantly increased in all osteoporotic studied groups compared to the group of healthy rats. However, the OP group had poor quality cortical bone [38]. Both bone mass and matrix structure (e.g., collagen mutations and minerals) contribute to bone strength [39]. The

current results have supported our recent study of OVX-d rats and GIOP rat models. We reported no significant differences between osteoporotic (OVX-d and GIOP) rats and healthy rats in terms of high stress load [23].

OP is a disease that results in decreased bone density and deterioration of bone structure [40]. Bisphosphonates are currently used as first-line therapeutic agents for OP. Bisphosphonates inhibit bone resorption by selective adsorption to mineral surfaces and subsequent internalization by bone-resorbing osteoclasts where they interfere with various biochemical processes. Alendronate inhibits a key enzyme, farnesyl pyrophosphate synthase, in the mevalonate pathway and thereby prevents the biosynthesis of isoprenoid compounds considered essential for post-translational modification of small guanosine triphosphate (GTP)-binding proteins. Both protein prenylation and function of these regulatory proteins are impaired, leading to osteoclast dysfunction [41]. In support, the current study results have shown that alendronate

Fig. 5 Mean \pm SEM of the total bone marrow volume (mm^3) of the studied groups compared by Mann-Whitney test (for nine groups) and LSD test (for OVX-d groups); $*p < 0.05$; $**p < 0.01$. The OC group showed the lowest bone marrow volume among the studied groups. There were significant differences between the OC group and the DC, OA, and OL groups

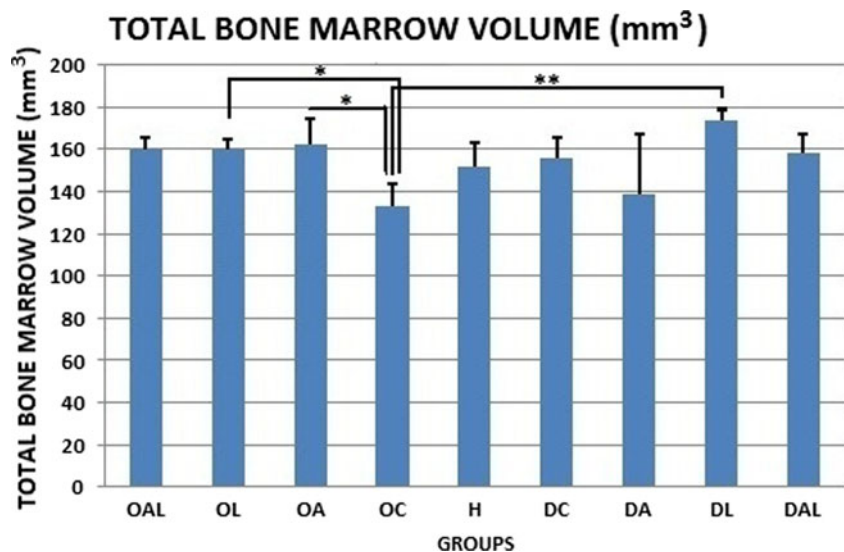
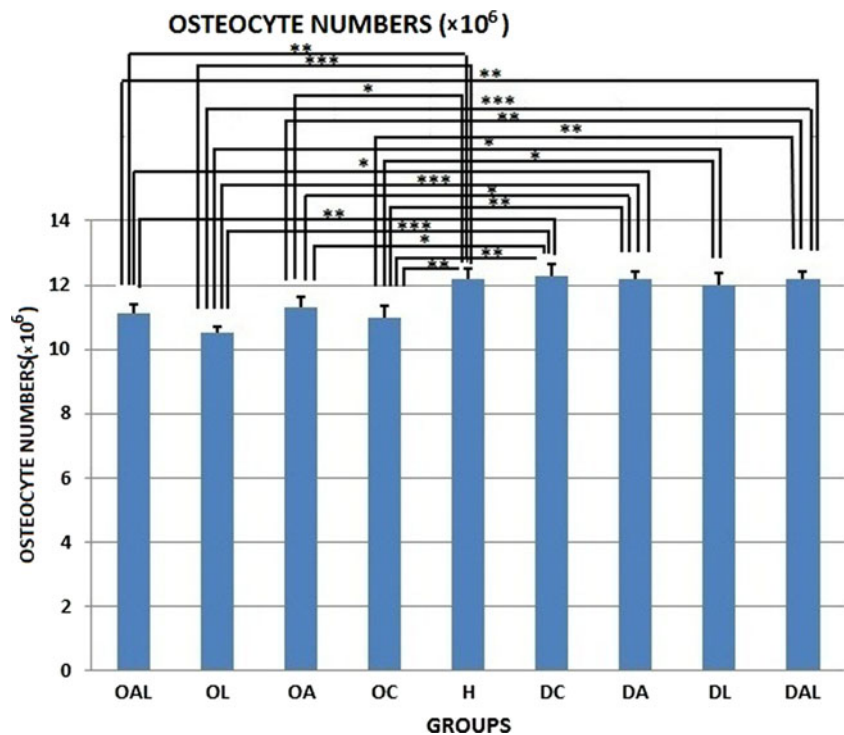


Fig. 6 Mean \pm SEM of osteocyte numbers ($\times 10^6$) of the studied groups compared by LSD test; * $p < 0.05$; ** $p < 0.01$; *** $p < 0.001$. There was a significant decrease in osteocyte number in the OA, OC, OL, and OAL groups compared to the healthy group. The dexamethasone-treated rats showed a significant increase in osteocyte number compared to the OVX-d rats



alone or in combination with PW LLLT significantly decreased osteoclast numbers compared to their control groups.

We observed that PW LLLT did not significantly reverse the adverse effects observed in the tibias of OVX-d and GIOP rats. These results agreed with previous findings [21]. Muniz Renno et al. investigated the effects of CW LLLT on the femurs from OVX-d rats that exercised. The rats underwent an exercise program and laser irradiation for 48 h during 8 weeks. The laser irradiation was performed using an aluminum gallium arsenide (AlGaAs) laser (830 nm, 100 W/cm², 120 J/cm², Teralaser, DMC, São Carlos, SP, Brazil). There were greater bone strength and physical properties in the exercised animals.

However, LLLT did not show any synergistic effect with exercise on osteoporotic rats. Medalha et al. studied the effects of electrical stimulation and LLLT on bone loss in a rat model of spinal cord injury in four groups of rats: standard control, spinal cord-injured control (SC), spinal cord-injured rats treated with laser (SCL, GaAlAs, 830 nm, CW, 30 mW/cm², 250 J/cm²), and spinal cord-injured rats subjected to electrical field stimulation (SCE, 1.5 MHz, 1:4 duty cycles, 30 mW, 20 min). The SC rats displayed a marked decrease in bone mass, biomechanical properties, and morphometric parameters versus the standard control group. The SCE rats had higher tibial diaphysis areas and inner tibial diameters compared with the

Fig. 7 Mean \pm SEM of the osteoblast numbers ($\times 10^6$) of the studied groups compared by Mann-Whitney test; ** $p < 0.01$. There was a significant decrease in osteoblast number in the OA, OC, and OL groups compared to the healthy group. The DA, DL, and DAL groups showed a significant increase in osteoblast number compared to the OC, OA, and OL groups

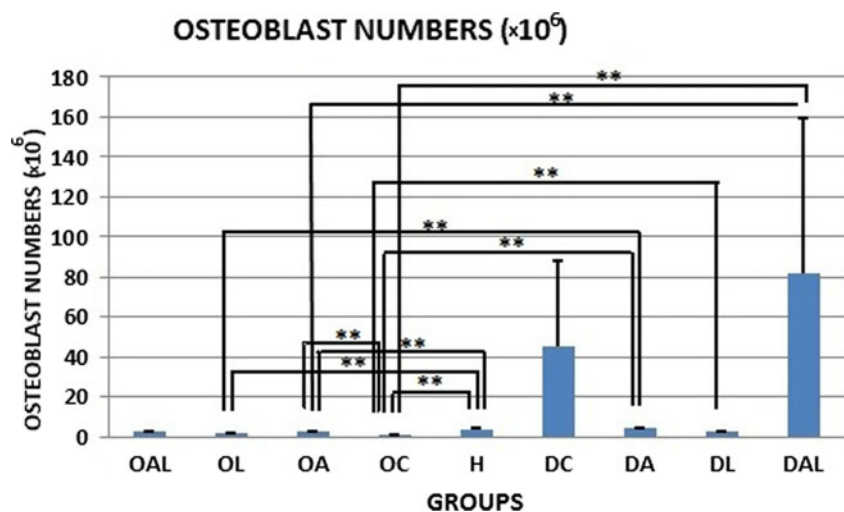
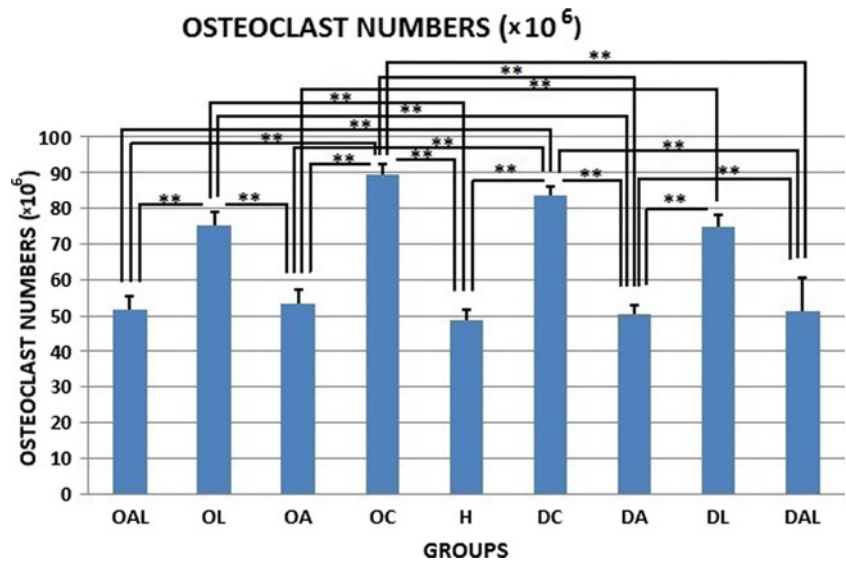


Fig. 8 Mean ± SEM of the osteoclast numbers ($\times 10^3$) of the studied groups compared by Mann-Whitney test; $**p < 0.01$. The healthy group showed the lowest number of osteoclasts among the studied groups. The OC and DC groups showed significant increases in osteoclast number compared to most other groups



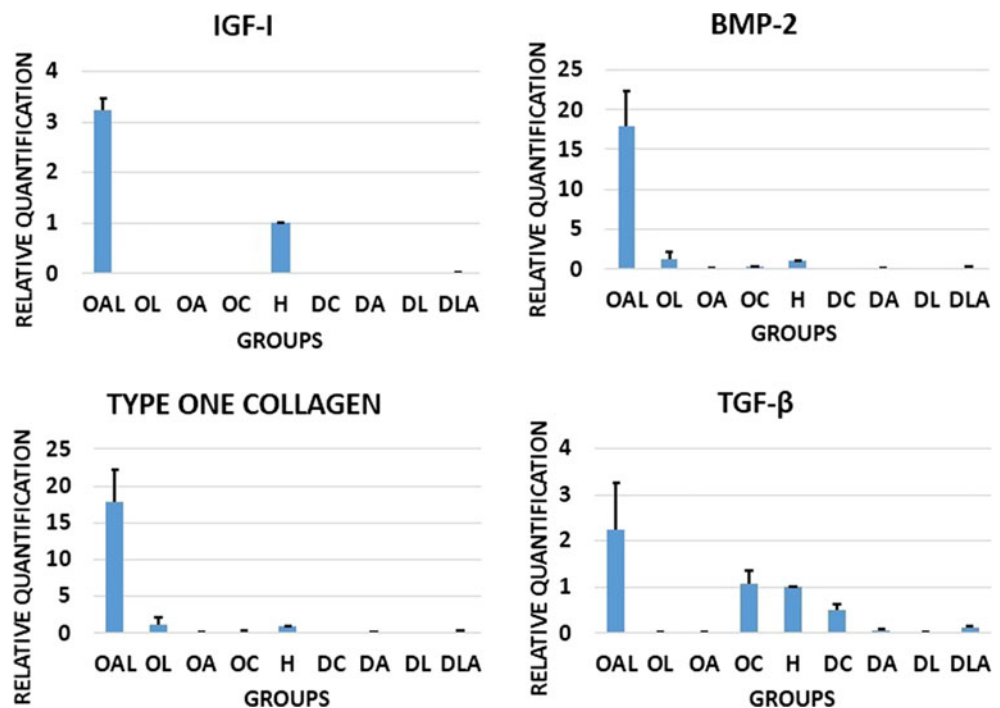
SC group. Results for the SCL group demonstrated a trend toward the SC group results. They observed no increase in either mechanical or densitometric parameters [22].

We observed that PW LLLT did not adequately reduce the damage in ovariectomized rats with OP that received dexamethasone. The combination of alendronate and PW LLLT in OVX-d rats and GIOP rats significantly decreased osteoclast numbers in the osteoporotic tibias compared to the control groups. The results of this study agreed with a study by Diniz et al. [42]. These researchers investigated the effect of CW LLLT in combination with bisphosphonate on osteoporotic trabecular bone structure [42]. LLLT was performed

using a Ga-Al-As laser (830 nm, 50 mW, 4 J/cm²) on the neck of the femur and the vertebral body. Surprisingly, in the association between laser and alendronate, the trabecular bone volume was significantly greater in the vertebrae.

Muniz Renno et al. investigated the effects of an 830-nm infrared LLLT on bone properties and bone strength of the rats femurs after OVX. In their study, LLLT had a preventive impact on bone loss in rats after OVX. The result of this study contrasted the results reported by Renno et al. [20]. The reason for this discrepancy might be attributed to differences in the methodology. They initiated laser irradiation 1 day after OVX at a dose of 120 J/cm², and LLLT was performed three times a

Fig. 9 Mean ± SEM of mRNA levels of TGF-beta, IGF-I, BMP-2, and type 1 collagen of studied groups compared by Mann-Whitney test. Real-time PCR analysis revealed that there were no significant differences of mRNA gene expression of TGF-beta, IGF-I, BMP-2, and type 1 collagen among the studied groups



week for 2 months after which the femurs were submitted to a biomechanical test and evaluation of physical properties [20].

Recently, a number of studies have investigated the effects of LLLT on the repair process of osteoporotic fractures. Some authors reported that laser irradiation alone accelerated the initial phase of the repair process [43], inhibited the inflammatory process, and induced cell proliferation [44]. Scalize et al. reported that LLLT (20 and 30 J/cm²) improved bone formation in osteoporotic rats. They observed significantly more new bone formation in the groups that received 20 and 30 J/cm² compared to the control groups. These researchers used stereological parameters to evaluate the repair process in osteoporotic fractures [45]. The effects of 50 mJ/cm² [43] and 133 J/cm² [44] on the repair process of osteoporotic fractures were evaluated by histological analysis [43, 44]. Other studies that focused on the use of bone scaffolds in addition to morphometrical and biomechanical evaluating methods reported conflicting results. Bossini et al. reported that LLLT irradiation in combination with Biosilicate® led to improvements in bone repair because it increased bone formation, deposition of collagen, and angiogenesis [46]. Fangel et al. investigated the effects of Biosilicate® and LLLT (60 J/cm²) on bone fracture consolidation in osteoporotic rats. They observed that the combination of LLLT with Biosilicate® improved bone formation, bone repair, and indentation values, as a biomechanical test [47]. Fangel et al., in another study, investigated the effects of LLLT and Biosilicate® on the biomechanical properties of the bone callus in osteoporotic rats. They concluded that Biosilicate® alone or in association with LLLT improved the biomechanical properties of the tibial bone callus in these rats [48].

Three hypotheses that attempt to explain the lack of a stimulatory effect of PW LLLT on osteoporotic rats can be suggested. First, this finding could be due to the deep, systemic effects of OP on bone. It seems possible that the OVX-d and GIOP models used in the current study were so profound that the osteoporotic bone tissue was not able to respond properly to any stimulation (PW LLLT or alendronate). Another possibility could be the PW LLLT parameters employed in this study. The applied dose was selected in accordance with two studies which demonstrated that an 890-nm infrared laser at 0.972 J/cm² increased bone strength in healthy rats [23, 49]. Finally, the use of LLLT has been shown to rely to a large extent on the local effects of lights on the tissues [50, 51]; however, OP is a systemic disease.

Conclusion

The OVX-d and GIOP animal OP models used in this study had negative effects on bone tissue. Alendronate significantly

decreased osteoclast numbers in osteoporotic rats. Concurrent treatments of PW LLLT and alendronate produced the same effect on osteoporotic bone. Since the PW LLLT has osteogenic effects, different parameters should be investigated to verify whether an appropriate PW LLLT protocol in combination with a proper(s) anti-osteoporotic agent(s) might reverse the detrimental effects of OP.

Acknowledgments We wish to extend our sincere thanks to the late Mrs. Jamileh Rezaei. This article was financially supported by the Research Department of the School of Medicine and the Vice Chancellor of Research at Shahid Beheshti University of Medical Sciences, Tehran, Iran (grants: 1393-1-91-1350 and 1392-1-115-1160).

Compliance with ethical standards

Conflict of interest The authors declare that they have no conflict of interest.

Animal rights and informed consent All procedure were approved by the Medical Ethics Committee at Shahid Beheshti University of Medical Sciences, Tehran, Iran (Protocols no.:1393-1-91-1350 and 1392-1-115-1160).

References

1. Johnell O, Kanis J (2006) An estimate of the worldwide prevalence and disability associated with osteoporotic fractures. *Osteoporos Int* 17(12):1726–1733
2. Syddall HE, Evandrou M, Dennison EM, Cooper C, Sayer AA (2012) Social inequalities in osteoporosis and fracture among community-dwelling older men and women: findings from the Hertfordshire Cohort Study. *Arch Osteoporos* 7(1–2):37–48
3. Lewiecki EM, Laster AJ (2006) Clinical applications of vertebral fracture assessment by dual-energy x-ray absorptiometry. *J Clin Endocrinol Metab* 91(11):4215–4222
4. Abrahamsen B, Van Staa T, Ariely R, Olson M, Cooper C (2009) Excess mortality following hip fracture: a systematic epidemiological review. *Osteoporos Int* 20(10):1633–1650
5. Riggs BL, Khosla S, Melton LJ 3rd (2002) Sex steroids and the construction and conservation of the adult skeleton. *Endocr Rev* 23(3):279–302
6. Burr DB, Turner CH, Naick P, Forwood MR, Ambrosius W, Hasan MS, Pidaparti R (1998) Does microdamage accumulation affect the mechanical properties of bone? *J Biomech* 31(4):337–345
7. Dai R-C, Liao E-Y, Yang C, Wu X-P, Jiang Y (2004) Microcracks: an alternative index for evaluating bone biomechanical quality. *J Bone Miner Metab* 22(3):215–223
8. Braidman IP, Hainey L, Batra G, Selby PL, Saunders PT, Hoyland JA (2001) Localization of estrogen receptor β protein expression in adult human bone. *J Bone Miner Res* 16(2):214–220
9. Hughes DE, Dai A, Tiffée JC, Li HH, Mundy GR, Boyce BF (1996) Estrogen promotes apoptosis of murine osteoclasts mediated by TGF- β . *Nat Med* 2(10):1132–1136
10. McNamara L (2010) Perspective on post-menopausal osteoporosis: establishing an interdisciplinary understanding of the sequence of

- events from the molecular level to whole bone fractures. *J R Soc Interface* 7(44):353–372
11. Khosla S, Westendorf JJ, Oursler MJ (2008) Building bone to reverse osteoporosis and repair fractures. *J Clin Invest* 118(2):421–428
 12. Reddy GK (2004) Photobiological basis and clinical role of low-intensity lasers in biology and medicine. *J Clin Laser Med Surg* 22(2):141–150
 13. van Brussel MS, Bultink IE, Lems WF (2009) Prevention of glucocorticoid-induced osteoporosis. *Expert Opin Pharmacother* 10(6):997–1005
 14. Cashman KD (2007) Diet, nutrition, and bone health. *J Nutr* 137(11):2507S–2512S
 15. Sohn H, Ko Y, Park M, Kim D, Moon YL, Jeong YJ, Lee H, Moon Y, Jeong BC, Kim O, Lim W (2015) Effects of light-emitting diode irradiation on RANKL-induced osteoclastogenesis. *Lasers Surg Med* 22(10):22413
 16. Kiyosaki T, Mitsui N, Suzuki N, Shimizu N (2010) Low-level laser therapy stimulates mineralization via increased Runx2 expression and ERK phosphorylation in osteoblasts. *Photomed Laser Surg* 28(1)
 17. Shimizu N, Mayahara K, Kiyosaki T, Yamaguchi A, Ozawa Y, Abiko Y (2007) Low-intensity laser irradiation stimulates bone nodule formation via insulin-like growth factor-I expression in rat calvarial cells. *Lasers Surg Med* 39(6):551–559
 18. Ko CY, Kang H, Seo DH, Jung B, Schreiber J, Kim HS (2013) Low-level laser therapy using the minimally invasive laser needle system on osteoporotic bone in ovariectomized mice. *Med Eng Phys* 35(7):1015–1019
 19. Kang H, Ko CY, Ryu Y, Seo DH, Kim HS, Jung B (2012) Development of a minimally invasive laser needle system: effects on cortical bone of osteoporotic mice. *Lasers Med Sci* 27(5):965–969
 20. Renno AC, de Moura FM, dos Santos NS, Tirico RP, Bossini PS, Parizotto NA (2006) Effects of 830-nm laser light on preventing bone loss after ovariectomy. *Photomed Laser Surg* 24(5):642–645
 21. Muniz Renno AC, de Moura FM, dos Santos NS, Tirico RP, Bossini PS, Parizotto NA (2006) The effects of infrared-830 nm laser on exercised osteopenic rats. *Lasers Med Sci* 21(4):202–207
 22. Medalha CC, Amorim BO, Ferreira JM, Oliveira P, Pereira RM, Tim C, Lirani-Galvao AP, da Silva OL, Renno AC (2010) Comparison of the effects of electrical field stimulation and low-level laser therapy on bone loss in spinal cord-injured rats. *Photomed Laser Surg* 28(5):669–674
 23. Fridoni M, Masteri Farahani R, Nejati H, Salimi M, Gharavi SM, Bayat M, Amini A, Torkman G, Bayat S (2015) Evaluation of the effects of LLLT on biomechanical properties of tibial diaphysis in two rat models of experimental osteoporosis by a three point bending test. *Lasers Med Sci* 30(3):1117–1125
 24. Kanis J, McCloskey E, Johansson H, Cooper C, Rizzoli R, Reginster J-Y (2013) European guidance for the diagnosis and management of osteoporosis in postmenopausal women. *Osteoporos Int* 24(1):23–57
 25. Li X, Ominsky MS, Warmington KS, Niu QT, Asuncion FJ, Barrero M, Dwyer D, Grisanti M, Stolina M, Kostenuik PJ, Simonet WS, Paszty C, Ke HZ (2011) Increased bone formation and bone mass induced by sclerostin antibody is not affected by pretreatment or cotreatment with alendronate in osteopenic, ovariectomized rats. *Endocrinology* 152(9):3312–3322
 26. Ferretti JL, Gaffuri O, Capozza R, Cointry G, Bozzini C, Olivera M, Zanchetta JR, Bozzini CE (1995) Dexamethasone effects on mechanical, geometric and densitometric properties of rat femur diaphyses as described by peripheral quantitative computerized tomography and bending tests. *Bone* 16(1):119–124
 27. Sun P, Cai DH, Li QN, Chen H, Deng WM, He L, Yang L (2010) Effects of alendronate and strontium ranelate on cancellous and cortical bone mass in glucocorticoid-treated adult rats. *Calcif Tissue Int* 86(6):495–501
 28. Sterio D (1984) The unbiased estimation of number and sizes of arbitrary particles using the disector. *J Microsc* 134(2):127–136
 29. Gundersen HJ, Jensen EB, Kieu K, Nielsen J (1999) The efficiency of systematic sampling in stereology—reconsidered. *J Microsc* 193(Pt 3):199–211
 30. Gundersen HJ, Bendtsen TF, Korbo L, Marcussen N, Moller A, Nielsen K, Nyengaard JR, Pakkenberg B, Sorensen FB, Vesterby A et al (1988) Some new, simple and efficient stereological methods and their use in pathological research and diagnosis. *APMIS* 96(5):379–394
 31. Gundersen H-JG (1986) Stereology of arbitrary particles. *J Microsc* 143(1):3–45
 32. Livak KJ, Schmittgen TD (2001) Analysis of relative gene expression data using real-time quantitative PCR and the 2^{-ΔΔCT} method. *Methods* 25(4):402–408
 33. Yeh JK, Chen MM, Aloia JF (1996) Ovariectomy-induced high turnover in cortical bone is dependent on pituitary hormone in rats. *Bone* 18(5):443–450
 34. Jagtap VR, Ganu JV, Nagane NS (2011) BMD and serum intact osteocalcin in postmenopausal osteoporosis women. *Indian J Clin Biochem* 26(1):70–73
 35. Green D, Wallace H (2003) Late effects of childhood cancer. CRC Press
 36. Parfitt AM (1987) Trabecular bone architecture in the pathogenesis and prevention of fracture. *Am J Med* 82(1B):68–72
 37. Lane NE, Yao W, Balooch M, Nalla RK, Balooch G, Habelitz S, Kinney JH, Bonewald LF (2006) Glucocorticoid-treated mice have localized changes in trabecular bone material properties and osteocyte lacunar size that are not observed in placebo-treated or estrogen-deficient mice. *J Bone Miner Res* 21(3):466–476
 38. Chao EY, Inoue N, Koo TK, Kim YH (2004) Biomechanical considerations of fracture treatment and bone quality maintenance in elderly patients and patients with osteoporosis. *Clin Orthop Relat Res* 425:12–25
 39. Roschger P, Rinnerthaler S, Yates J, Rodan G, Fratzl P, Klaushofer K (2001) Alendronate increases degree and uniformity of mineralization in cancellous bone and decreases the porosity in cortical bone of osteoporotic women. *Bone* 29(2):185–191
 40. Oei L, Zillikens MC, Rivadeneira F, Oei EH (2015) Osteoporotic vertebral fractures as part of systemic disease. *J Clin Densitom*
 41. Russell RG (2007) Bisphosphonates: mode of action and pharmacology. *Pediatrics* 119(2):S150–S162
 42. Diniz JS, Nicolau RA, de Melo Ocarino N, do Carmo Magalhaes F, de Oliveira Pereira RD, Serakides R (2009) Effect of low-power gallium-aluminum-arsenic laser therapy (830 nm) in combination with bisphosphonate treatment on osteopenic bone structure: an experimental animal study. *Lasers Med Sci* 24(3):347–352
 43. Pires-Oliveira DA, Oliveira RF, Amadei SU, Pacheco-Soares C, Rocha RF (2010) Laser 904 nm action on bone repair in rats with osteoporosis. *Osteoporos Int* 21(12):2109–2114
 44. Re Poppi R, Da Silva AL, Nacer RS, Vieira RP, de Oliveira LV, Santos de Faria Junior N, de Tarso Camilo Carvalho P (2011) Evaluation of the osteogenic effect of low-level laser therapy (808 nm and 660 nm) on bone defects induced in the femurs of female rats submitted to ovariectomy. *Lasers Med Sci* 26(4):515–522
 45. Scalize PH, de Sousa LG, Regalo SC, Semprini M, Pitol DL, da Silva GA, de Almeida CJ, Coppi AA, Laad AA, Prado KF, Siessere

- S (2015) Low-level laser therapy improves bone formation: stereology findings for osteoporosis in rat model. *Lasers Med Sci* 30(5): 1599–1607
46. Bossini PS, Rennó AC, Ribeiro DA, Fangel R, Peitl O, Zanotto ED, Parizotto NA (2011) Biosilicate® and low-level laser therapy improve bone repair in osteoporotic rats. *J Tissue Eng Regen Med* 5(3):229–237
47. Fangel R, Bossini PS, Renno AC, Ribeiro DA, Wang CC, Toma RL, Nonaka KO, Driusso P, Parizotto NA, Oishi J (2011) Low-level laser therapy, at 60 J/cm² associated with a Biosilicate® increase in bone deposition and indentation biomechanical properties of callus in osteopenic rats. *J Biomed Opt* 16(7):3598847
48. Fangel R, Bossini PS, Renno AC, Granito RN, Wang CC, Nonaka KO, Driusso P, Parizotto NA, Oishi J (2014) Biomechanical properties: effects of low-level laser therapy and Biosilicate® on tibial bone defects in osteopenic rats. *J Appl Biomater Funct Mater* 12(3):271–277
49. Freidouni M, Nejati H, Salimi M, Bayat M, Amini A, Noruzian M, Asgharie MA, Rezaian M (2015) Evaluating glucocorticoid administration on biomechanical properties of rats' tibial diaphysis. *Iran Red Crescent Med J* 17(3)
50. Chow RT (2000) Dose dilemmas in low level laser therapy—the effects of different paradigms and historical perspectives. *Laser Therapy* 13(1):102–109
51. Bayat M, Ansari E, Gholami N, Bayat A (2007) Effect of low-level helium–neon laser therapy on histological and ultrastructural features of immobilized rabbit articular cartilage. *J Photochem Photobiol B Biol* 87(2):81–87